Eur. Phys. J. A **28**, 83–89 (2006)
DOI 10.1140/epja/i2005-10275-y

THE EUROPEAN PHYSICAL JOURNAL A

Is there a hadron spin-flip contribution to the Coulomb-hadron interference at small momentum transfer and high energies?

O.V. Selyugin[a]

BLTPh, JINR, Dubna, Russia

Received: 21 December 2005 / Revised version: 16 March 2006 /
Published online: 26 May 2006 –
Communicated by Xiangdong Ji

Abstract. The analysing power A_N is examined in the range of the Coulomb-hadron interference on the basis of the experimental data from $p_L = 6\,\mathrm{GeV}/c$ up to $200\,\mathrm{GeV}/c$ taking account of a phenomenological analysis at $p_L = 6\,\mathrm{GeV}/c$ and a dynamic high-energy spin model. The results are compared with the new RHIC data at $p_L = 100\,\mathrm{GeV}/c$. The new experimental data obtained at RHIC indicate small contributions of the hadron spin-flip amplitude.

PACS. 11.80.Cr Kinematical properties (helicity and invariant amplitudes, kinematic singularities, etc.) – 13.85.Dz Elastic scattering

1 Introduction

Most of the recent experiments require a very accurate knowledge of the polarization of beams. This especially relates to the large spin programs at RHIC. These programs include measurements of the spin correlation parameters in the diffraction range of elastic proton-proton scattering. There is a proposal to use the Coulomb-nucleon interference (CNI) effects [1] to measure the beam polarization [2] very exactly and quickly. This effect appears from the interference of the imaginary part of the hadron spin–non-flip amplitude and the real part of the electromagnetic spin-flip amplitude determined by the charge-magnetic moment interaction. Now new very precise experimental data are obtained at RHIC [3,4].

Determination of the structure of the hadron scattering amplitude is an important task for both theory and experiment. Perturbative quantum chromodynamics cannot be used in calculation of the real and imaginary parts of the scattering amplitude in the diffraction range. A worse situation is for the spin-flip parts of the scattering amplitude in the domain of small momentum transfer. On the one hand, the usual representation says that the spin-flip amplitude dies at superhigh energies, and, on the other hand, we have different non-perturbative models which lead to a non-dying spin-flip amplitude at superhigh energies [5–7].

Note that the interference of the hadronic and electromagnetic amplitudes may give an important contribution not only at very small momentum transfer [8] but also in the range of the diffraction minimum [9]. However, for that one should know the phase of the interference of the Coulombic and hadronic amplitude at sufficiently large momentum transfer too.

Before the RHIC experiments, experimental data on the measurement of the spin correlation parameters at very small momentum transfer were very poor except for the unique experiment [10] having large errors though. After the first paper [11] a number of papers appeared which considered these questions and tried to estimate a possible contribution of the hadron spin-flip amplitude to the CNI effect [12–14].

Our difficulty mostly comes from the lack of experimental data at high energies and small momentum transfer. We should examine the available experimental data at different energies and in different domains of momentum transfer. In most analyses the experimental data at $p_L = 45.5\,\mathrm{GeV}/c$ and with $0.06 < |t| < 0.5\,\mathrm{GeV}^2$ and the data at $p_L = 200\,\mathrm{GeV}/c$ with $0.003 < |t| < 0.05$ are used. These experimental data overlap on the axis of momentum transfer but are measured at different energies. In most analyses the energy difference of all parameters determining the scattering amplitude is not considered. Of course, we have plenty of experimental data in the domain of small momentum transfer at low energies $3 < p_L < 12$ (GeV/c).

At these energies we have many contributions to the hadron spin-flip amplitudes coming from different regions of exchange. Now we cannot exactly calculate all contributions and find their energy dependence. However, a great amount of the experimental material allows us to make full phenomenological analyses, and obtain the size and form of the different parts of the hadron scattering amplitude.

[a] e-mail: selugin@theor.jinr.ru

The difficulty is that we do not know the energy dependence of these amplitudes and individual contributions of the asymptotic non-dying spin-flip amplitudes. As was noted in [15], the spin-dependent part of the interaction in pp scattering is stronger than expected and a good fit to the data in the Regge model requires an enormous number of poles.

Usually, one makes the assumptions that the imaginary and real parts of the spin–non-flip amplitude have an exponential behavior with the same slope and the imaginary and real parts of the spin-flip amplitudes, without the kinematic factor $\sqrt{|t|}$ [16]. For example, in [11] the spin-flip amplitude was chosen in the form

$$F_h^{fl} = \sqrt{-t}/m_p(b+ia)\,\mathrm{Im}\,F_h^{nf}. \tag{1}$$

That is not so as regards the t-dependence shown in ref. [13], where F_h^{fl} multiply the exponential form by the special function dependent on t. Moreover, one mostly takes the energy independence of the ratio of the spin-flip parts to the spin–non-flip parts of the scattering amplitude. All this is our theoretical uncertainty [17,18].

2 Model approximation

In [19], the phenomenological analysis of the experimental data was carried out to estimate the size of the hadron spin-flip amplitude from the experimental data on differential cross-sections, the influence of the hadron spin-flip amplitude on the CNI effect and a possibility of estimating this contribution from the experimental data on the measurement of the analyzing power in the nucleon-nucleon elastic scattering. Now we can compare those results with the new experimental data obtained at RHIC.

The differential cross-sections measured in an experiment are described by the square of the scattering amplitude which is used to fit experimental data determining the electromagnetic and hadron amplitudes and the Coulomb-hadron phase.

For the electromagnetic helicity amplitudes, one takes the usual one-photon approximations (see [20,21]):

$$\begin{aligned} F_{1,3}^{em}(t) &= \frac{\alpha}{t}\, f_1(t)^2, \\ F_2^{em}(t) &= -F_4^{em}(t) = \alpha\, f_2^2(t), \\ F_5^{em}(t) &= -\frac{\alpha}{\sqrt{|t|}}\, f_1(t)\, f_2(t) \end{aligned} \tag{2}$$

with

$$\begin{aligned} f_1(t) &= \frac{4\,m_p^2 - (\mu_p - 1)\,t}{4\,m_p^2 - t}\, G_D, \\ f_2(t) &= \frac{2\,m_p\,(\mu_p - 1)}{4\,m_p^2 - t}\, G_D, \\ G_D(t) &= \frac{1}{1 - t/0.71^2}, \\ \mu_p &= 2.793, \qquad m_p = 0.93827\,\mathrm{GeV}. \end{aligned} \tag{3}$$

As a result, the total helicity amplitudes can be written as

$$F_i(s,t) = F_i^H(s,t) + F_i^{em}(t)e^{-i\alpha\varphi(s,t)}, \tag{4}$$

with the Coulomb-hadron phase [9] calculated for the whole diffraction range taking into account the hadron form-factors. The differential cross-sections and spin correlation parameters are

$$\frac{\mathrm{d}\sigma}{\mathrm{d}t} = 2\pi\left(|F_1|^2 + |F_2|^2 + |F_3|^2 + |F_4|^2 + 4|F_5|^2\right), \tag{5}$$

$$A_N\frac{\mathrm{d}\sigma}{\mathrm{d}t} = -4\pi\,\mathrm{Im}[(F_1 + F_2 + F_3 - F_4) * F_5^*). \tag{6}$$

We shall restrict our discussion to the analysis of A_N. In the standard pictures the spin-flip and double spin-flip amplitudes correspond to the spin-orbit (LS) and spin-spin (SS) coupling terms. The contribution to A_N from the hadron double spin-flip amplitudes already at $p_L = 6\,\mathrm{GeV}/c$ is of the second order compared to the contribution from spin-flip amplitude. So, with the usual high-energy approximation for the helicity amplitudes at small momentum transfer we suppose that $F_1 = F_3$ and we can neglect the contributions of the hadron parts of $F_2 - F_4$. Note that if F_1, F_3, F_5 have the same phases, their interference contribution to A_N will be zero, though the size of the hadron spin-flip amplitude can be large. Hence, if these phases have a different s- and t-dependence, the contribution from the hadron spin-flip amplitude in A_N can be zero at s_i, t_i and non-zero at other s_j, t_j. It means that the comparison of the size of $A_N(s)$ at one t_i, as made for example in [22], at different s makes a strong assumption about the energy independence of many different parameters determining the size of $A_N(s,t)$.

The analysing power corresponding to the pure electromagnetic-hadron interference (with $F_5^H = 0$) will be denoted by A_N^{CH}. Its size is proportional, in the major part, to the interference of the imaginary part of the hadron spin–non-flip amplitude with the real part of the electromagnetic spin-flip amplitude. Note that there is also a small contribution from the interference of the real and imaginary parts of the above-mentioned amplitudes.

The existing experimental data at sufficiently high energy show the significant size of A_N in the t-region of the dip of the differential cross-sections. At the present moment, we have, as has been noted above, that in some models the hadron asymptotic spin-flip amplitude is not dying at superhigh energy. However, most part of the experimental data of the analyzing power lies at low energies. Hence, we should take the low-energy amplitudes and build a continuous transition to the asymptotic amplitudes.

As asymptotic amplitudes let us take those calculated in the dynamical model (DM) [7]. In [23] on the basis of sum rules it has been shown that the main contribution to a hadron interaction at large distances comes from the triangle diagram with the 2π-meson exchange in the t-channel. As a result, the hadron amplitude can be represented as a sum of central and peripheral parts of the interaction

$$F(s,t) \propto F_c(s,t) + F_p(s,t), \tag{7}$$

where $F_c(s,t)$ describes the interaction between the central parts of hadrons; and $F_p(s,t)$ is the sum of the contributions of diagrams corresponding to the interactions of the central part of one hadron with the meson cloud of the other. The contribution of these diagrams to the scattering amplitude with an $N(\Delta$-isobar) in the intermediate state looks like [7]

$$F^{\lambda_1\lambda_2}_{N(\Delta)}(s,t) = \frac{g^2_{\pi NN(\Delta)}}{i(2\pi)^4}\int \mathrm{d}^4 q F_{\pi N}(s',t) \times \frac{\varphi_{N(\Delta)}[(k-q)^2,q^2]\varphi_{N(\Delta)}[(p-q)^2,q^2]}{[q^2-M^2_{N(\Delta)}+i\epsilon]} \times \frac{\Gamma^{\lambda_1\lambda_2}(q,p,k,)}{[(k-q)^2-\mu^2+i\epsilon][(p-q)^2-\mu^2+i\epsilon]}\,. \quad (8)$$

Here λ_1 and λ_2 are the helicities of nucleons, $F_{\pi N}$ is the πN-scattering amplitude, Γ is a matrix element of the numerator of the diagram representation, φ are vertex functions chosen in the dipole form with the parameters $\beta_{N(\Delta)}$:

$$\varphi_{N(\Delta)}\big(l^2, q^2 \propto M^2_{N(\Delta)}\big) = \frac{\beta^4_{N(\Delta)}}{(\beta^2_{N(\Delta)} - l^2)^2}. \quad (9)$$

The model with the N and Δ contribution provides a self-consistent picture of the differential cross-sections and spin phenomena of different hadron processes at high energies. Really, parameters in the amplitude determined from, for example, elastic pp scattering, allow one to obtain a wide range of results for elastic meson-nucleon scattering and charge-exchange reaction $\pi^- p \to \pi^0 n$ at high energies.

It is essential that the model predicts large polarization effects for all considered reactions at high and superhigh energies [7]. The predictions are in good agreement with the experimental data in the energy region available for experiment. Also note that just the effect of large distances determines a large value of the spin-flip amplitude of the charge-exchange reaction [24].

The results weakly depend on the model for the spin–non-flip amplitude. Different models must give the same differential cross-sections in a wide range of momentum transfer and energies. Moreover, they must describe the energy dependence of $\rho(s) = \mathrm{Re}\,F(s,0)/\,\mathrm{Im}\,F(s,0)$. Basically, only the behavior of the real part of the spin–non-flip amplitudes in the range of the diffraction minimum may depend on the model and leads to different predictions. In this paper, we consider a usual picture of the proton-proton and proton-antiproton cross-sections with the crossing symmetry fulfilled.

As a low-energy amplitude let us take the one obtained in [15] where the full analysis of experimental data was carried out and the full set of the helicity spin amplitudes and their eikonals of the proton-proton scattering at $p_L = 6\,\mathrm{GeV}/c$ was extracted. Let us take the eikonal of the spin-non-flip amplitudes in a form similar to the form and size obtained in [15] at $p_L = 6\,\mathrm{GeV}/c$:

$$1 - e^{\chi_c(b)} = h_1 e^{-c_1 b^2} - h_2 e^{-c_2 b^2} + h_3 e^{-c_3 b^2} + i\left(h_4 e^{-c_4 b^2} - h_5 e^{-c5 b^2} + h_6 e^{-c_6 b^2}\right) \quad (10)$$

and for the hadron spin-flip amplitude

$$\chi_{ls}(b) = h_{ls}\big[1 + b\; e^{\mu(s)(b-b_0)}\big]^{-1}, \quad (11)$$

where h_i, c_i, h_{ls} and b_0 are the parameters obtained in ref. [15]. As we know, these amplitudes reproduce the analyzing power at $p_L = 6\,\mathrm{GeV}/c$. In fact, these amplitudes are the sum of terms falling, constant and growing with energy. However, this form has no energy dependence of the parameters which change the form of these amplitudes with increasing energy in both the spin–non-flip and spin-flip parts. To obtain the energy dependence of some part of the amplitudes (10), (11), let us multiply (11) by the falling term s_1/s and take into account the change of the form of (11) with energy; let us introduce the energy dependence into the parameter $\mu \to \mu_s$:

$$\mu(s) = \mu_0(\log s_0/\log s), \quad (12)$$

where $s_0 = 13.152\,\mathrm{GeV}$ corresponds to $p_L = 6\,\mathrm{GeV}/c$ and μ_0 corresponds to the values of ref. [15].

The DM amplitude also includes the falling, constant, and increasing terms, but it is not suitable for describing low-energy data. So it is not a simple task to sew these two amplitudes together, the low-energy phenomenological one and the high-energy model. To obtain a smooth transform to the DM representation, let us multiply these amplitudes by the factor-functions $fs^{nf,fl}_{ex}$ quickly decreasing with energy, and multiply the DM amplitudes by the factor-functions $f^{nf,fl}_{th}$

$$fs^{nf}_{ex}(s) = \exp\big[-(s/s^{nf})^2 + (s_0/s^{nf})^2\big],$$
$$fs^{nf}_{th}(s) = 1 - \exp\big[-(s/s^{nf})^2 + (s_0/s^{nf})^2\big]; \quad (13)$$

$$fs^{fl}_{ex}(s) = \exp\big[-(s/s^{fl})^2 + (s_0/s^{fl})^2\big],$$
$$fs^{nf}_{th}(s) = 1 - \exp\big[-(s/s^{fl})^2 + (s_0/s^{fl})^2\big], \quad (14)$$

where $s_0 = 13.152\,\mathrm{GeV}$ corresponds to $p_L = 6\,\mathrm{GeV}/c$. In this case, we obtain that the analyzing power at $p_L = 6\,\mathrm{GeV}/c$ is described only by the amplitudes obtained in ref. [15] and at superhigh energies only by the DM amplitude. In the domain of approximately $6 \le p_L \le 200\,\mathrm{GeV}/c$ the analyzing power has both the contributions. The parameters s^{nf} and s^{fl} were chosen to obtain the description of experimental data available in this energy range: $s^{nf} = 40\,\mathrm{GeV}^2$, $s^{fl} = 64\,\mathrm{GeV}^2$. We do not carry out the fitting procedure. The values of these parameters were chosen to obtain a qualitative description of the polarization data at $p_L = 11.75\,\mathrm{GeV}/c$. We do not take into account the data of the differential cross-sections. However, to check our procedure we calculate the differential cross-sections at $p_L = 50\,\mathrm{GeV}/c$ and at $p_L = 100\,\mathrm{GeV}/c$ and compare them with the existing experimental data.

The calculated analyzing power at $p_L = 6\,\mathrm{GeV}/c$ is shown in fig. 1a. Of course, in the original phenomenological analysis made in [15] all helicity amplitudes were used, but it can be seen that a good description, practically the same as in [15], of experimental data on the analyzing power can be reached only with one hadron spin-flip amplitude.

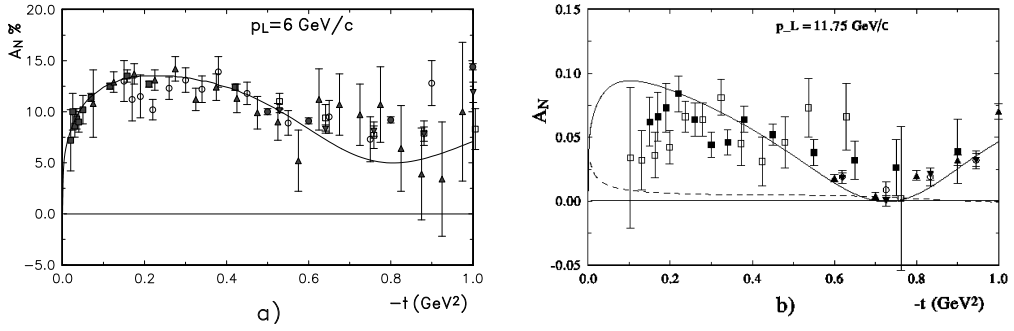

Fig. 1. The analyzing power A_N of the pp scattering calculated a) at $p_L = 6\,\mathrm{GeV}/c$ (experimental data from [25,26]), and b) at $p_L = 11.75\,\mathrm{GeV}/c$ (experimental data from [26,27]).

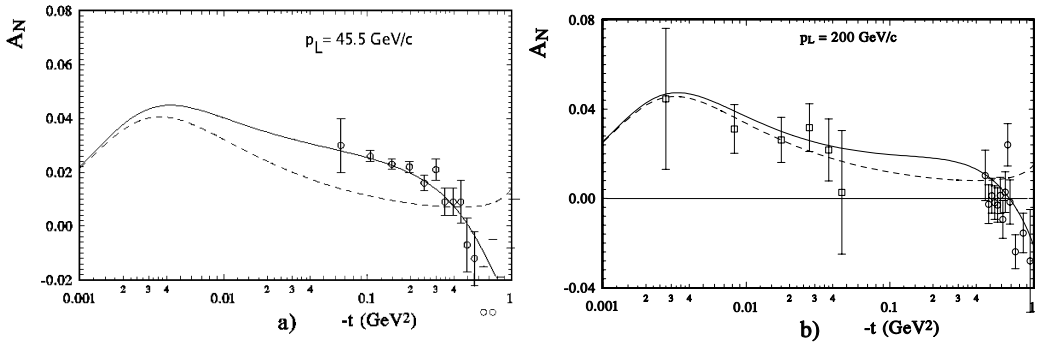

Fig. 2. The analyzing power A_N of the pp scattering calculated a) at $p_L = 45.5\,\mathrm{GeV}/c$ (experimental data from [28]), and b) at $p_L = 200\,\mathrm{GeV}/c$ (experimental data from [29,30]).

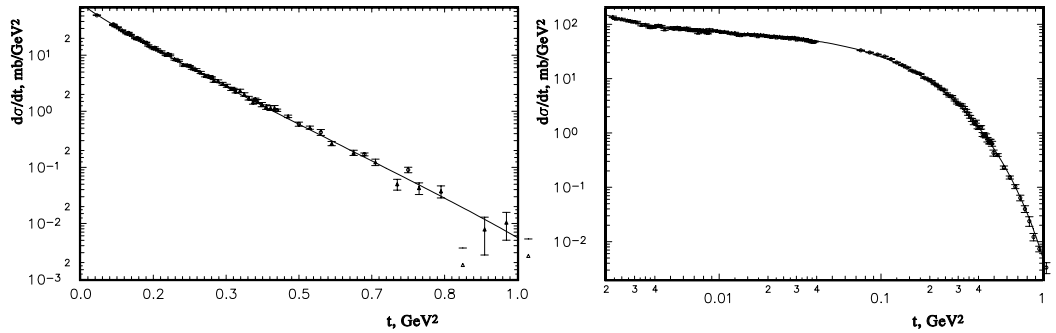

Fig. 3. The differential cross-sections of the pp scattering calculated at $p_L = 50\,\mathrm{GeV}/c$ (left) (experimental data from [31,32]) and at $p_L = 100\,\mathrm{GeV}/c$ (right) (experimental data from [32,33]).

The experimental data at $p_L = 11.75\,\mathrm{GeV}/c$ seriously differ from those at $p_L = 6\,\mathrm{GeV}/c$ but our calculations reproduce them sufficiently well (fig. 1b). It is shown that our energy dependence was chosen correctly and we may hope that further on we will obtain correct values of the analyzing power.

Indeed, our calculations at $p_L = 45.5\,\mathrm{GeV}/c$ show a satisfactory description of the experimental data (see fig. 2a). At this energy both of our parts of the amplitude give important contributions. The contributions to the analyzing power of the amplitudes (10), (11) are approximately twice as large as the contributions of the model amplitudes. From fig. 2a we can see that in the region $|t| \approx 0.2\,\mathrm{GeV}^2$ the contributions from the hadron spin-flip amplitudes are most important.

At last, fig. 2b shows our calculations at $p_L = 200\,\mathrm{GeV}/c$. At this energy, the contributions of the phenomenological amplitudes are already very small and can be compared with the contributions of the model amplitudes only at $|t| = 0.5\,\mathrm{GeV}^2$ where both the contributions are very small.

Let us check how our amplitudes describe the differential cross-sections, especially for the intermediate region where both the solutions give one-order contributions. The calculations for $p_L = 50\,\mathrm{GeV}/c$ and $p_L = 100\,\mathrm{GeV}/c$ are presented in fig. 3. The non-normalized experimental data [32] were normalized to the experimental data [31] at $p_L = 50\,\mathrm{GeV}/c$ and [33] at $p_L = 100\,\mathrm{GeV}/c$. It is clear that the coincidence of the theoretical curves with experimental data is sufficiently good for both energies and the whole

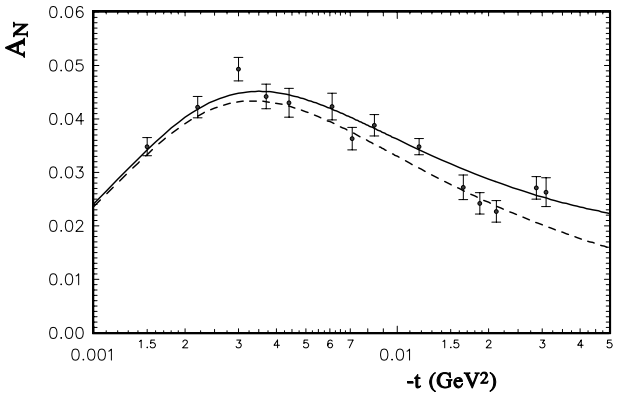

Fig. 4. The analyzing power A_N of the pp scattering calculated at $p_L = 100\,\mathrm{GeV}/c$; the full line is the model calculations; the dashed line is the model calculation of the A_N^{CH}.

examined region of momentum transfer. We would like to emphasize that we do not make a fit of the differential cross-sections. We only sew the low- and high-energy solutions [15] and [7]. The parameters of the factor-functions were chosen to obtain a qualitative description of the form of A_N at $p_L = 11.5\,\mathrm{GeV}/c$ and then they were fixed.

Note that we obtain a different energy dependence of the additional contributions ΔA_N to the pure A_N^{CH} effect at different points of momentum transfer. The contribution at $|t| = 0.1\,\mathrm{GeV}^2$ has a clear downfall with growing $\sqrt{s}$, but in the range of the maximum of A_N^{CH} we have nearly constant contributions which are independent of energy. So we cannot draw the conclusion about the energy dependence of ΔA_N at the maximum of A_N^{CH} measuring the energy dependence of the analyzing power at other points of the momentum transfer. However, it is one of the central points of many other analyses of the electromagnetic-hadron interference effect.

The comparison of our calculations with the recent final experimental data obtained at RHIC [34] (see fig. 4) at $p_L = 100\,\mathrm{GeV}/c$ shows suitable agreement. The preliminary experimental data were slightly above the final ones and showed, in our opinion, the existence of hadron spin-flip contributions. The final data, to say accurately, do not contradict such contributions. We will analyze the final data in the next section.

Especially note that it is very important to continue the measured range at the largest momentum transfer. In the future it is most important to measure A_N in the range of the dip of the differential cross-sections and high energies. The corresponding predictions were made in [35]. The value of r_5 —the ratio of the hadron spin-flip amplitude to the hadron spin–non-flip amplitude (without the kinematic factor $\sqrt{|t|}$) determined in [11] is

$$r_5 = 2m_p\ [\mathrm{Re}\, F^{+-} + i\,\mathrm{Im}\, F^{+-}]/(\sqrt{|t|}\,\mathrm{Im}\, F_h^{++}). \quad (15)$$

In our model calculations at $p_L = 100\,\mathrm{GeV}$ and at the position of the maximum A_N we obtain the value of r_5 $(p_L = 100\,\mathrm{GeV}, -t_{max}) = -0.015 - i0.01$. Of course, this value depends on both energy and momentum transfer. More complete analyses of these dependences were carried out in [19].

3 Phenomenological analysis of A_N^{CH}

There is one important note. In fig. 4 our curve for pure electromagnetic-hadron interference A_N^{CH} reaches at maximum the size 4.37%. On the contrary, in talks and publications, the preliminary new experimental data are compared with the curve of A_N^{CH} which reaches at its maximum approximately 4.77%. From the comparison of the curve with the new experimental data the authors draw a conclusion that the contribution from the hadron spin-flip amplitude disappears.

We study this problem to understand the contradiction with our calculations. Some authors suppose that the value A_N^{CH} does not practically depend on energy. In an early work [36], where the size of A_N^{CH} was evaluated, it was obtained that

$$A_N^{CH} \sim 4.5\%\ \mathrm{Im}(a_h)/|a_h|, \quad (16)$$

where a_h is a spin–non-flip amplitude. In the case of a small real part of a_h this form leads to a size of A_N^{CH} independent of the size of σ_{tot}. However, this formula gives a small dependence of the size of A_N^{CH} on the $\rho(s,t)$ —the ratio of the real to the imaginary part of the hadron spin–non-flip amplitude. Over a period of time this short version of A_N^{CH} was rewritten in different forms which led to a different energy dependence. Our opinion is that when we calculate such a small correlations effect we have to take the complete form of A_N^{CH}, formula (6). All the approximations must be reflected in the form of the helicity amplitudes and the size of the parameters.

There is an important energy dependence which is connected with the energy dependence of the Coulomb-hadron interference term in the differential cross-sections. This term is in most part proportional to the size of $\rho(s,t)$. The position of the maximum of the contribution of this term to the differential cross-section at t coincides approximately with the position of the maximum of A_N^{CH}.

Hence, the energy dependence of $\rho(s,t)$ strongly impacts that of the maximum of A_N^{CH} (see fig. 5). In our semi-phenome-nological descriptions we obtained the following values at $p_L = 100\,\mathrm{GeV}$: $\sigma_{tot} = 38.3\,\mathrm{mb}$, $B(-t = 0.003\,\mathrm{GeV}^2) = 11.6\,\mathrm{GeV}^{-2}$, $B(-t = 0.03) = 11.3\,\mathrm{GeV}^{-2}$, $\rho(-t = 0.003\,\mathrm{GeV}^2) = -0.105$.

The available experimental data (see [37]) are: $\sigma_{tot} = 38.46 \pm 0.04\,\mathrm{mb}$, $B(-t = 0.03) = 11.3\,\mathrm{GeV}^{-2}$, $\rho = -0.1$. So our values practically coincide with the existing experimental data.

Of course, there also exists an energy dependence of the Coulomb-hadron phase which impacts the size of the differential cross-sections. In our original calculation we used this phase, which was obtained in [9] with taking into account all correction factors. To check up the results, we used the simplest phase in the form of West-Yennie [38] and in the form of Cahn [39]

$$\varphi = -[\ln(B|t|/2) + \gamma + \ln(1 + 8/(B/L))], \quad (17)$$

Table 1.

n	Form of $F_i(s,t)$	σ_{tot} (mb)	ρ	k_i	k_r	$\sum_1^{14}\chi_i^2$
1a	exponential	38.46	-0.105	0	0	30.62
2a	exponential	38.46	-0.047 ± 0.02	0	0	23.22
3a	exponential	36.5 ± 0.81	-0.1	0	0	24
4a	model	38.3	-0.105	0	0	29.38
1b	model	38.3	-0.105	-0.065	-0.15	26.11
2b	exponential	38.46	-0.1	0.023 ± 0.06	-0.022 ± 0.02	20.64
3b	exponential	38.46	-0.1	0.02	0.023 ± 0.01	20.65
4b	exponential	38.46	-0.1	0.028 ± 0.01	0.0	20.95
5b	exponential	38.46	-0.091 ± 0.032	0.02	0.021 ± 0.014	20.58
6b	exponential	38.46	-0.1 ± 0.03	0.028 ± 0.015	0.0	20.58

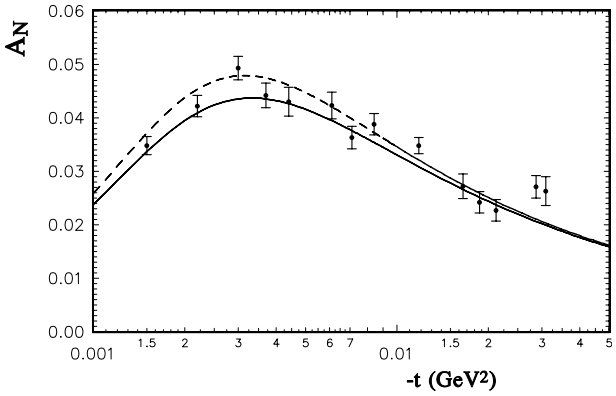

Fig. 5. The phenomenological A_N^{CH} for the pp scattering, calculated at $p_L = 100\,\mathrm{GeV}/c$ (the full and dashed lines are the calculations with $\rho = -0.1$ and with $\rho = 0$); experimental data from [4].

where B is the slope of the differential cross-sections and $L = 0.71$. The size of A_N^{CH} for our small momentum transfer region changes only by 0.5%.

Now let us obtain the result for A_N^{CH} with the simplest form of the hadron spin–non-flip amplitude:

$$F_h(s,t) = \frac{\sigma_{tot}(s)}{4\pi}\ (\rho + i)\ \exp(B(s)\ t/2) \qquad (18)$$

and with the Coulomb-hadron phase of (17). We take the hadron spin-flip amplitude in the form

$$F_h^{sf}(s,t) = \frac{\sigma_{tot}(s)}{4\pi}\ (k_r\rho + ik_i)\ \exp(B(s)\ t/2). \qquad (19)$$

First, let us make the fit of the experimental data without the hadron spin-flip amplitude. This case is presented in the upper part of table 1 (1a-4a). The fit with the parameters obtained in the model calculations but with the form of the amplitudes in the simple exponential form (18) is shown in the first row. If we take ρ as a free parameter, χ^2 essentially decreases but the size of ρ arrives at the value which strongly differs from the experimental data. The same situation is obtained if σ_{tot} is taken as a free parameter. The last row (4a) of the upper part of the table presents the calculation of χ^2 on the basis of the model calculations but without the hadron spin-flip contribution. Note that we did not make the variation of the parameters of our model calculations for that case. χ^2 was calculated by comparing the model calculations with the values of the experimental points.

In the lower part of table 1 (1b-6b) the different fits with the existence of the hadron spin-flip amplitude are presented. Again χ^2 on the basis of the model calculations with the hadron spin-flip contribution was calculated without variation of the parameters. In this case, χ^2 decreased by 4 units. A more remarkable decrease in χ^2 was obtained with variation of the parameters of the hadron spin-flip amplitude for the cases of the exponential form of the helicity amplitudes. Of course, when both the parameters k_r and k_i are varied, the errors are large (see line 2b in the table). If k_r is fixed to some value or zero, the errors in the determination of the imaginary part of the hadron spin-flip amplitude are 30%. It is to be noted that the coefficient k_r is multiplied by ρ in the definition of the real part of the hadron spin-flip amplitude. Hence, the ratio of the imaginary and real parts is practically the same for F_h^{nf} and F_h^{sf} but the signs are different, thus leading to a difference between the corresponding phases. As the fitting procedure shows, the small real part of F_h^{sf} can be taken with $k_r = 0$. In this case, k_i grows (line 4b in the table). It is interesting that if we make the fit of ρ and k_i simultaneously, the size of ρ practically does not change (see line 6b and compare it with line 2a).

4 Conclusion

The size of the parameters of the hadron spin-flip amplitude which can be obtained from the new experimental data at $p_L = 100\,\mathrm{GeV}/c$ is determined with large errors. However, χ^2 decreases appreciably. It is shown at least that the imaginary part of the hadron spin-flip amplitude differs from zero in this momentum transfer region for $p_L = 100\,\mathrm{GeV}/c$. Note that the imaginary part of the spin-flip amplitude gives a contribution not only to the interference with the hadron spin–non-flip amplitude but also to the interference with the Coulombic part. Hence, we cannot draw a conclusion about the absence of a contribution

to the hadron spin-flip amplitude at least on the basis of these new experimental data.

It is obvious from our analysis that examining the contributions of the hadron spin-flip amplitudes in the CNI effect using the experimental data in a wide energy region, one should take into account the energy dependence of all parts of the hadron scattering amplitude and its dependence on momentum transfer. Our descriptions of all available experimental data give about 3.5% of the predictions for RHIC energies for the contributions of the hadron spin-flip amplitude to the maximum of the CNI effect. Of course, this estimation is very rough, but the comparison of the calculated A_N and A_N^{CH} with the new experimental data obtained at RHIC shows that at this energy a contribution of the hadron spin-flip amplitude is present. More accurate estimations can be carried out only after a new experiment in this domain of transfer momenta at higher energies and wider momentum transfer, especially in the dip region.

The author acknowledges useful discussions with J.-R. Cudell and would like to thank the group of fundamental theoretical physics of the University of Liège for their hospitality and the FRNS for financial support.

References

1. J. Schwinger, Phys. Rev. **73**, 407 (1948); L.I. Lapidus, Nucl. Part. **9**, 84 (1978); N.H. Battimore, E. Gotsman, E. Leader, Phys. Rev. D **18**, 694 (1978).
2. N. Akchurin, A. Bravar, M. Conte, A. Penzo, University of Iowa Report 93-04; W. Guryn *et al.*, *Total and Differential Cross Sections and Polarization Effects in pp Elastic Scattering at RHIC*, unpublished; S.B. Nurushev, A.G. Ufimtsev, *Proceedings of Hera-N, Dubna*, edited by V.A. Korotkov, W.-D. Nowak, JINR E2-96-40 (1996), DESY-Zeuthen report 96-09 (1996); N.H. Battimore *et al.*, Phys. Rev D **59**, 114010 (1999).
3. A. Bravar *et al.*, in *Proceedings of the XVI International Symposium on High Energy Spin Physics, 10-16 October 2004, Trieste*, edited by K. Aulenbacher, F. Bradamante, A. Bressan, A. Martin, p. 700, ISBN 981-256-315-6 (1995); in *Proceedings of the X International Conference ADS, Blois* (2004); H. Okada *et al.*, p. 507, nucl-ex/0502022.
4. A. Bravar *et al.*, to be published in *Proceedings of the X EDS International Conference, 23-30 May 2005, Blois, France*; A. Bravar *et al.*, in *Proceedings of the XIV International Conference on High Energy Spin Physics, 27-30 September 2004, Dubna*, edited by O. Teryaev, A. Efremov, W. Haeberli (Cern Courier, October 2005) p. 15.
5. C. Bourrely, J. Soffer, T.T. Wu, Phys. Rev. D **19**, 3249 (1979).
6. B.Z. Kopeliovich, B.G. Zakharov, Phys. Lett. B **156**, (1989); M. Anselmino, S. Forte, Phys. Rev. Lett. **71**, 223 (1993); S.V. Goloskokov, Phys. Lett. B **315**, 459 (1993); A.E. Dorokhov, N.I. Kochelev, Yu.A. Zubov, Int. J. Mod. Phys. A **8**, 603 (1993).
7. S.V. Goloskokov, S.P. Kuleshov, O.V. Selyugin, Z. Phys. C **50**, 455 (1991).
8. J.R. Cudell, E. Predazzi, O.V. Selyugin, Part. Nucl. **36**, 132 (2004).
9. O.V. Selyugin, Int. J. Mod. Phys. A **12**, 1379 (1997);
10. N. Akchurin *et al.*, Phys. Rev. D **48**, 326 (1993).
11. N. Akchurin, N.H. Buttimore, A. Penzo, Phys. Rev. D **51**, 3944 (1995).
12. A.D. Krisch, S.M. Troshin, hep-ph/9610537.
13. C. Bourrely, J. Soffer, hep-ph/9611234.
14. N.H. Buttimore, *Proceedings of the XII High Energy Spin Physics, 10-14 September 1996, Amsterdam*, edited by C.W. Jager *et al.* (World Scientific, Singapore, 1997).
15. M. Sawamoto, S. Wakaizumi, Proc. Theor. Phys. **62**, 1293 (1979).
16. N.H. Buttimore *et al.*, Phys. Rev. D **59**, 114010 (1999).
17. J.-R. Cudell, E. Predazzi, O.V. Selyugin, Eur. Phys. J. A **21**, (2004); hep-ph/0401040.
18. A.F. Martin, E. Predazzi, Phys. Rev. D **66**, 034029 (2002).
19. O.V. Selyugin, Phys. At. Nucl. **62**, 333 (1999).
20. S. Gasiorowicz, *Elementary Particle Physics* (John Wiley & Sons, Inc, New York - London - Sydney, 1967).
21. V. Barone, E. Predazzi, in *High Energy Particle Diffraction* (New York, 2002).
22. T.L. Trueman, hep-ph/9610429.
23. S.V. Goloskokov, S.P. Kuleshov, O.V. Selyugin, Yad. Fiz. **46**, 597 (1987).
24. S.V. Goloskokov, S.P. Kuleshov, O.V. Selyugin, Yad. Fiz. **52**, 561 (1990).
25. D. Miller *et al.*, Phys. Rev. D **16**, 2016 (1977); M. Borghini *et al.*, Phys. Lett. B **31**, 405 (1970); R. Diebold *et al.*, Phys. Rev. Lett. **35**, 632 (1975); D.R. Rust *et al.*, Phys. Lett. B **58**, 114 (1975); R.D. Klem *et al.*, Phys. Rev. D **15**, 602 (1977); J.R. O'Fallon *et al.*, Phys. Rev. D **17**, 24 (1978).
26. M. Borghini *et al.*, Phys. Lett. B **24**, 77 (1966).
27. S.L. Kramer *et al.*, Phys. Rev. D **17**, 1709 (1978); K. Abe *et al.*, Phys. Lett. B **63**, 239 (1976).
28. A. Gaudot *et al.*, Phys. Lett. B **61**, 103 (1976).
29. G. Fidegaro *et al.*, Phys. Rev. B **105**, 309 (1981).
30. E.L. Berger *et al.*, Phys. Rev. D **17**, 2971 (1978).
31. D.S. Ayres *et al.*, Phys. Rev. D **15**, 3105 (1977).
32. C.W. Akerlof *et al.*, Phys. Rev. D **14**, 2864 (1976).
33. J.P. Burq *et al.*, Nucl. Phys. B **217**, 285 (1983).
34. H. Okada *et al.*, hep-ph/0601001.
35. N. Akchurin, S.V. Goloskokov, O.V. Selyugin, Int. J. Mod. Phys. A **14**, 252 (1999).
36. A.P. Vanzha, L.I. Lapidus, A.V. Tarasov, Yad. Fiz. **16**, 1023 (1972); B.Z. Kopeliovich, L.I. Lapidus, Yad. Fiz. **19**, 218 (1974).
37. Landolt-Börnstein, New Ser., Vol. **9** (1980).
38. G.B. West, D.R. Yennie, Phys. Rev. **172**, 1414 (1968).
39. R.N. Cahn, Z. Phys. C **15**, 253 (1982).